Measurement of finite frequency noise cross-correlations with a resonant circuit

Marjorie Creux, Adeline Crépieux, Thierry Martin

Measurement of finite frequency noise cross-correlations with a resonant circuit

M. Creux, A. Crépieux, and T. Martin

Centre de Physique Théorique, Case 907 Luminy,

13288 Marseille cedex 9, France and

Université de la Méditerranée, 13288 Marseille cedex 9, France

(Dated: July 29, 2005)

Abstract

The measurement of finite frequency noise cross-correlations represents an experimental challenge in mesoscopic physics. Here we propose a generalisation of the resonant LC circuit setup of Lesovik and Loosen which allow to probe directly such cross-correlations by measuring the charge fluctuations on the plates of a capacitor. The measuring circuit collects noise contributions at the resonant frequency of the LC circuit. Auto-correlation noise can be canceled out by switching the wires and making two distinct measurements. The measured cross-correlations then depend of four non-symmetrized correlators. This detection method is applied to a normal metal three terminal device. We subsequently discuss to what extent the measurement circuit can detect electron-antibunching and what singularities appear in the spectral density of noise cross-correlations.

PACS numbers:

I. INTRODUCTION

The measurement of finite frequency noise in mesoscopic systems provides a useful diagnosis of the carriers involved in the transport. In normal metal conductors, finite frequency correlations exhibit a singularity at $\omega = eV$[1, 2], in normal-supraconductor junctions, Andreev reflexion gives rise to a singularity at $2eV$[3] signaling that Cooper pairs enter the superconductor, in the fractional quantum Hall effect, the tunneling of quasiparticles in the vicinity of a point contact leads to a singularity at $e\nu V$[4], with ν the filling factor. At the same time, zero frequency noise cross correlations can be used to probe directly the statistics of the charge carriers: are the carriers bunched or anti-bunched[5]? This implies a "Y" geometry where carriers are injected in one arm, and correlations are measured in the two receiving arms. While several proposals have appeared in order to measure two terminal noise with an auxiliary mesoscopic circuit (see below), to this date no equivalent proposal has been made for noise cross-correlations. The purpose of the present paper is to propose to fill this gap, using a resonant circuit[6].

Provided that an experimentalist includes in his/her setup appropriate electronics which can sample the current at discreet times, finite frequency noise can in principle be computed directly from this time series. Here however, we focus on an apparatus – a measuring device coupled to the mesoscopic device – which provides a direct probe of its noise. There are essentially two such types of proposals for measuring auto-correlations: inductive coupling and capacitive coupling. The proposal of Lesovik and Loosen[6] consists of a LC circuit coupled inductively to the fluctuating current emanating from a mesoscopic conductor: the measurement of the charge fluctuations on the capacitor plates provides a measurement of the noise at the resonant frequency of the circuit. Aguado and Kouvenhoven[7] have proposed to measure the noise of an arbitrary circuit by coupling capacitively this circuit to a detector circuit: an inelastic current flows in the detector circuit when a "photon" $\hbar\omega$ which corresponds to the level structure of the measurement device is provided by the mesoscopic circuit. This theoretical suggestion has been successfully implemented to measure the finite frequency noise of a Josephson junction using a large Superconductor-Insulator-Suprerconductor junction[8]: quasiparticles tunnelling in the SIS junction can occur only if it is assisted by the frequency provided by the antenna.

Zero frequency noise cross-correlations have obvious applications in the study of Hanbury–Brown and Twiss experiments in nanoelectronics. However, in recent years finite frequency

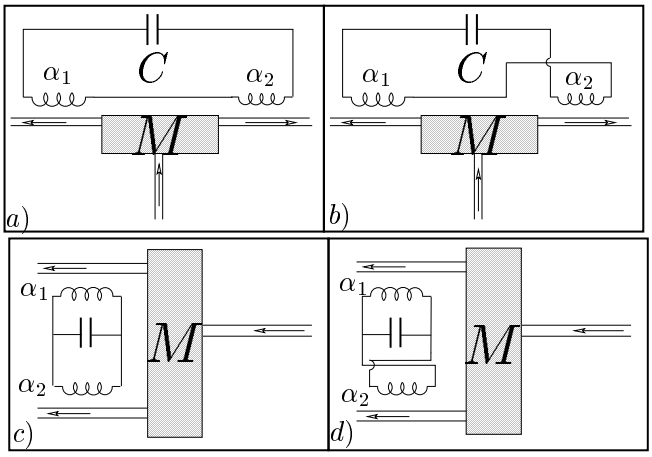

FIG. 1: Schematic description of the noise cross-correlation setup. M is the mesoscopic circuit to be measured, C is the capacitor and there are two inductors with coupling constants α_1 and α_2 to the mesoscopic circuit. a) and b): the electrical components of the detector are in series and they "see" the current with the same sign (a) or with the opposite sign (b). c) and d): the electrical components of the detector are in parallels and they "see" the current with the same sign (c) or with the opposite sign (d).

noise cross-correlations have been shown to also play an important role. An example is in the study of electronic entanglement[9, 10], another is in the identification of anomalous charges in Luttinger liquid wires[11], which will be discussed below.

The paper is organized as follows. In section II, the model is introduced, and it is shown how cross-correlations can be directly obtained. In section III, we compute the measured cross-correlation noise. Our results are then applied in section IV to a simple device: a three terminal normal metallic sample, where we stress the difference between the symmetrized noise, the non-symmetrized noise, and the measured noise. Section V gives two examples where cross-correlations are needed. We conclude in section VI.

II. MODEL AND METHOD

For measuring cross-correlations, two inductances (L_1 and L_2) and a single capacitor (C) are needed. The two inductors, which each have inductive coupling constants α_1 and α_2, are placed next to the two outgoing arms of the three terminal mesoscopic device (Fig. 1). We consider two cases: the two inductances are placed in series (Fig. 1a and Fig. 1b) or in

parallel (Fig. 1c and Fig. 1d). Depending on the wiring of these inductances (Fig. 1a,c or Fig. 1b,d), the two inductances "see" the outgoing currents with the opposite sign or with the same sign. Classically, the charge x on the capacitor plates of the measuring circuit obeys the equation of motion:

$$M\ddot{x}(t) = -Dx(t) - \alpha_1 \dot{I}_1(t) \mp \alpha_2 \dot{I}_2(t) \ , \tag{2.1}$$

where the "mass" $M = L_1 + L_2$ if the circuit is in series (Fig. 1a,b) or $M = L_1 L_2/(L_1 + L_2)$ if the circuit is in parallel (Fig. 1c,d), and $D = 1/C$. The currents which appear in the two coupling terms are $I_{1(2)}(t) = l^{-1} \int_{x_{1(2)}-l/2}^{x_{1(2)}+l/2} I(r,t)dr$, where l the length of the inductive coupling region. The characteristic frequency of the LC circuit is $\Omega = \sqrt{D/M}$.

The derivation of Ref. 6 is generalized to the two inductance situation. To quantize the measuring circuit, we note that the equation of motion can be derived from the Hamiltonian:

$$H = H_0 + H_{int} = \frac{p^2}{2M} + \frac{Dx^2}{2} + H_{int} \ , \tag{2.2}$$

with

$$H_{int} = x(\alpha_1 \dot{I}_1(t) \pm \alpha_2 \dot{I}_2(t)) \ . \tag{2.3}$$

The mesoscopic circuit plus measuring circuit are assumed to be decoupled at $t = -\infty$. The coupling between the two is switched on adiabatically, and one can monitor the moments of the charge of capacitor in the presence of the fluctuating currents at time $t = 0$: it is a stationary measurement.

The n-th power of the capacitor charge reads, in the interaction representation:

$$\langle x^n(0) \rangle = Tr[e^{-\beta H_0} U^{-1}(0) x^n(0) U(0)] \ , \tag{2.4}$$

with the evolution operator

$$U(0) = T \exp\left(\frac{-i}{\hbar} \int_{-\infty}^{0} dt' H_{int}(t') \right) \ . \tag{2.5}$$

We calculate perturbatively the n-th power of the charge, expanding the evolution term $(U(0))$ in powers of H_{int}. Considering the average charge and its square, one obtains:

$$\langle x(0) \rangle = \langle x(0) \rangle_1 + \langle x(0) \rangle_3 + ... \tag{2.6}$$

$$\langle x^2(0) \rangle = \langle x^2(0) \rangle_0 + \langle x^2(0) \rangle_2 + ... \tag{2.7}$$

where the different orders in H_{int} are linked to the higher cumulants of the current: $\langle x(0)\rangle_1$ contains information about the average current, $\langle x^2(0)\rangle_2$ about the current fluctuations, and $\langle x(0)\rangle_3$ about the third moment, and so on.

The zero order contribution of the charge fluctuation gives:

$$\langle x^2(0)\rangle_0 = \frac{\hbar}{2M\Omega}(N(\Omega)+1/2)\ , \tag{2.8}$$

with $N(\omega) = 1/(e^{\beta\hbar\Omega}+1)$ is the Bose Einstein distribution at the detector circuit temperature, which is not necessarily the mesoscopic device temperature. The next non-vanishing term, which depends on products of current operators is:

$$\begin{aligned}\langle x^2(0)\rangle_{2\pm} = \quad & \Big\langle \frac{1}{2}\Big(\frac{-i}{\hbar}\Big)^2 \int_{-\infty}^{0} dt_1 \int_{-\infty}^{t_1} dt_2 \\ \times \ & \Big[[x(0), x(t_1)(\alpha_1 \dot{I}_1(t_1) \pm \alpha_2 \dot{I}_2(t_1))], \\ & x(t_2)(\alpha_1 \dot{I}_1(t_2) \pm \alpha_2 \dot{I}_2(t_2))\Big] \Big\rangle\ ,\end{aligned} \tag{2.9}$$

where one recalls that the sign in front of the coupling constants $\alpha_{1,2}$ reflect the choice of the circuit, (a or b) and (c or d). The calculation of the charge fluctuations gives four terms: two autocorrelation terms which correspond to the fluctuations due to a single inductor (in terms of α_1^2 or α_2^2), and two terms associated with the correlation between the two inductors, which are proportional to $\alpha_1\alpha_2$. It is precisely these latter terms which allow to detect the noise correlations. Thus, it seems that it is impossible in practice to get rid of the autocorrelation terms: the measurement of the cross terms would require a prior knowledge of the charge fluctuations for a single impedance with a high degree of accuracy. We argue that this is not the case, provided that two measurements with the same setup but with different wiring can be achieved. One measures the charge fluctuations $\langle x^2(0)\rangle_{2+}$ with the geometry of Fig. 1a for the inductances in series (Fig. 1c for the parallel case), and subsequently one can switch the wiring and measure such fluctuations $\langle x^2(0)\rangle_{2-}$ with the circuit of Fig. 1b (Fig. 1d). In each case (series or parallel setup) by subtracting the two signals:

$$\langle x^2(0)\rangle_2 = \frac{1}{2}\big(\langle x^2(0)\rangle_{2+} - \langle x^2(0)\rangle_{2-}\big)\ , \tag{2.10}$$

one isolates the contribution of cross-correlations, which is proportional to $\alpha_1\alpha_2$. The combination of current cross-correlators will be referred from now on as the measured cross correlations.

III. MEASURED CROSS-CORRELATIONS AND NON-SYMMETRIZED NOISE

In order to proceed, the charge is now written in terms of the oscillator variables of the LC circuit:

$$x(t) = \sqrt{\frac{\hbar}{2M\Omega}}(ae^{-i\Omega t} + a^\dagger e^{i\Omega t}) \ , \tag{3.1}$$

where a is the destruction operator which satisfies $\langle a^\dagger a\rangle = N(\Omega)$. The first commutator in Eq. (2.9) becomes:

$$[x^2(0), x(t_1)\dot{I}_i(t_1)] = \Big(\frac{\hbar}{2M\Omega}\Big)^{3/2} 4i\sin(\Omega t_1)(a + a^\dagger)\dot{I}_i(t_1) \ , \tag{3.2}$$

and the average of the two interlocked correlators of Eq. (2.9) reads:

$$\begin{aligned}\Big\langle\Big[[x^2(0), x(t_1)\dot{I}_i(t_1)], x(t_2)\dot{I}_j(t_2)\Big]\Big\rangle &= \Big(\frac{\hbar}{M\Omega}\Big)^2 i\sin(\Omega t_1) \\ \times\ \Big\{&\langle\dot{I}_i(t_1)\dot{I}_j(t_2)\rangle\big[(N(\Omega)+1)e^{i\Omega t_2} + N(\Omega)e^{-i\Omega t_2}\big] \\ &-\langle\dot{I}_j(t_2)\dot{I}_i(t_1)\rangle\big[N(\Omega)e^{i\Omega t_2} + (N(\Omega)+1)e^{-i\Omega t_2}\big]\Big\} \ ,\end{aligned} \tag{3.3}$$

with $i, j = 1, 2$ $(i \neq j)$. Substituting this commutator in the expression of charge fluctuations, four correlators of current derivatives appear in the result. Translationnal invariance motivates the change of variables: $\{t_1, t_2\} \rightarrow \{t = t_1 - t_2, T = t_1 + t_2\}$. The charge fluctuations become:

$$\begin{aligned}\langle x^2(0)\rangle = \frac{\alpha_1\alpha_2}{(4M\Omega)^2}&\int_{-\infty}^{+\infty} dt \int_{-\infty}^{0} dT e^{\eta T} \\ \times\ \Big\{&(e^{i\Omega t} - e^{-i\Omega T sign(t)}) \\ &\times[(N(\Omega)+1)(\langle\dot{I}_2(0)\dot{I}_1(t)\rangle + \langle\dot{I}_1(0)\dot{I}_2(t)\rangle) \\ &-N(\Omega)(\langle\dot{I}_1(t)\dot{I}_2(0)\rangle + \langle\dot{I}_2(t)\dot{I}_1(0)\rangle)]\Big\} \ .\end{aligned} \tag{3.4}$$

In a manner similar to Refs. 6 and 12, the following non-symmetrized current correlators are introduced in Fourier space:

$$S_{ij}^+(\omega) \ = \ \int \frac{dt}{2\pi} e^{i\omega t}\langle I_i(0)I_j(t)\rangle \ , \tag{3.5}$$

$$S_{ij}^-(\omega) \ = \ \int \frac{dt}{2\pi} e^{i\omega t}\langle I_i(t)I_j(0)\rangle \ . \tag{3.6}$$

Translation invariance relates these two correlators: $S_{ij}^-(\omega) = S_{ij}^+(-\omega)$, and furthermore $\langle I_i(t_+)I_j(t_+)\rangle = \delta(t_+ - t_+)S_{ij}(t_+)$. Inserting the Fourier transform of the current $I_i(t)$

$\int d\omega I_i(\omega)e^{i\omega t}$ in the correlator for the derivative of the current, one obtains:

$$\langle \dot{I}_i(0)\dot{I}_j(t)\rangle \;=\; \int d\omega\omega^2 S^+_{ij}(\omega)e^{-i\omega t}\;, \tag{3.7}$$

$$\langle \dot{I}_i(t)\dot{I}_j(0)\rangle \;=\; \int d\omega\omega^2 S^-_{ij}(\omega)e^{-i\omega t}\;. \tag{3.8}$$

At this point, both integrals in Eq. (3.4) can be performed. The integration over t gives two contributions: one is a delta function, and the other gives products of principal parts, which cancel out. The charge fluctuations take the final form:

$$\begin{aligned}\langle x^2(0)\rangle \;=\; &\frac{\pi\alpha_1\alpha_2}{2\eta(2M)^2}\left[(N(\Omega)+1)(S^+_{12}(\Omega)+S^+_{21}(\Omega))\right.\\ &\left.-N(\Omega)(S^-_{12}(\Omega)+S^-_{21}(\Omega))\right]\;.\end{aligned} \tag{3.9}$$

This is a central result of this paper, which is illustrated below for a specific mesoscopic circuit. A similar result was mentioned in Ref. 13, although without justification. Note that the final result still depends on the adiabatic coupling parameter. In order to eliminate the dependence on η, the calculation can be generalized to a system with a distribution of oscillators, peaked around Ω. This is discussed in the appendix. The fact that the LC circuit has a finite line shape has of course a physical origin: the LC circuit contains dissipative elements, but for simplicity we do not consider the detailed mechanism for dissipation here.

IV. APPLICATION TO A THREE TERMINAL NORMAL CONDUCTOR

In a system of three terminals (Fig 2), a so called "Y junction", electrons are injected from terminal 1, which has a higher chemical potential than terminals 2 and 3. The noise cross–correlations are measured. This is the setup where the fermionic Hanbury–Brown and Twiss experiment[14] was proposed[5] and measured experimentally[15]. Without loss of generality, one considers that the three bias voltages, $\mu_{ij} = \mu_i - \mu_j$, $(i,j = 1,2,3)$, are chosen such that $\mu_{13} > \mu_{12}, \mu_{23}$.

Using scattering theory, one can readily obtain the general expression for the non-symmetrized finite frequency noise[16]:

$$\begin{aligned}S^+_{\alpha\beta}(\omega) \;=\; &\frac{e^2}{2\pi\hbar}\sum_{\gamma\delta}\int dE\;(\delta_{\alpha\gamma}\delta_{\alpha\delta} - s^\dagger_{\alpha\gamma}(E)s_{\alpha\delta}(E-\hbar\omega))\\ &\times(\delta_{\beta\delta}\delta_{\beta\gamma} - s^\dagger_{\beta\delta}(E)s_{\beta\gamma}(E-\hbar\omega))\\ &\times f_\gamma(E)(1-f_\delta(E-\hbar\omega))\end{aligned} \tag{4.1}$$

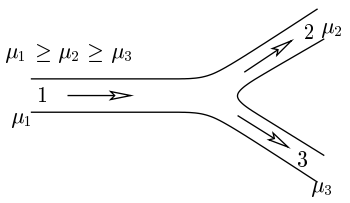

FIG. 2: A system with three terminals (Y junction) with chemical potentials μ_1, μ_2 and μ_3 with $\mu_1 \geq \mu_2 \geq \mu_3$.

where Greek letters represent the terminals and $s_{\alpha,\beta}$ is the scattering amplitude for electrons incoming from β and ending in α. $f_\gamma(E)$ is the Fermi-Dirac distribution function associated with terminal γ whose chemical potential is μ_γ. In what follows we assume that the temperature is much smaller than the applied biases. Here, one also neglects the energy dependence of the scattering matrix over the energy ranges specified by the voltages biases μ_{ij}. Furthermore, Eq. (4.1) neglects $\pm 2k_F$ oscillating terms in the noise fluctuations spectrum: this assumes that the region over which current is measured is much larger than the Fermi wave length, $l \gg \lambda_F$.

For $\mu_{23} < \mu_{12}$ and at negative frequencies, cross-correlations between terminals 2 and 3 yield:

$$S_{23}^{+}(\omega) \;=\; S_{32}^{+}(\omega) = -\frac{e^2}{2\pi}\omega(T_{21}T_{13} - (2 - R_2 - R_3)T_{23}) \\ -\frac{e^2}{2\pi\hbar}\begin{cases} (-\hbar\omega)(2T_{13}R_3 + 2T_{12}R_2 + 2T_{23}R_2) & \text{if } \hbar\omega < -\mu_{13} \\ T_{13}R_3(\mu_{13} - \hbar\omega) - \hbar\omega(2T_{12}R_2 + 2T_{23}R_2) & \text{if } -\mu_{13} < \hbar\omega < -\mu_{12} \\ T_{13}R_3(\mu_{13} - \hbar\omega) + T_{12}R_2(\mu_{12} - \hbar\omega) - \hbar\omega(2T_{23}R_2) & \text{if } -\mu_{12} < \hbar\omega < -\mu_{23} \\ T_{23}R_2(\mu_{23} - \hbar\omega) + T_{13}R_3(\mu_{13} - \hbar\omega) + T_{12}R_2(\mu_{12} - \hbar\omega) & \text{if } -\mu_{23} < \hbar\omega < 0 \end{cases} \tag{4.2}$$

while for positive frequencies:

$$S_{23}^{+}(\omega) \;=\; S_{32}^{+}(\omega) = -\frac{e^2}{2\pi\hbar}\begin{cases} T_{23}R_2(\mu_{23} - \hbar\omega) + T_{13}R_3(\mu_{13} - \hbar\omega) + T_{12}R_2(\mu_{12} - \hbar\omega) & \text{if } 0 < \hbar\omega < \mu_{23} \\ T_{13}R_3(\mu_{13} - \hbar\omega) + T_{12}R_2(\mu_{12} - \hbar\omega) & \text{if } \mu_{23} < \hbar\omega < \mu_{12} \\ T_{13}R_3(\mu_{13} - \hbar\omega) & \text{if } \mu_{12} < \hbar\omega < \mu_{13} \\ 0 & \text{if } \mu_{13} < \hbar\omega \end{cases} \tag{4.3}$$

where $R_\alpha = s_{\alpha,\alpha}^{\dagger} s_{\alpha,\alpha}$ is the reflexion probability from lead α and $T_{\alpha\beta} = s_{\alpha,\beta}^{\dagger} s_{\alpha,\beta} = T_{\beta\alpha}$ is the transmission probability from α to β.

As expected, the frequency dependence is given by a set of continuous straight lines with singular derivatives. At zero frequency, the non-symmetrized cross-correlations are:

$$S_{23}^{+}(\omega=0) \;=\; -\frac{e^2}{2\pi\hbar}(T_{23}R_2\mu_{23}+T_{13}R_3\mu_{13} + T_{12}R_2\mu_{12})\;. \tag{4.4}$$

The cross-correlations are negative regardless of bias voltage and transmission of the sample: one recovers the result of Ref. 5.

On the other hand, the symmetrized finite frequency cross-correlations are defined by:

$$S_{23}^{S}(\omega)=\int d\omega e^{i\omega t}\langle \Delta I_2(t)\Delta I_3(0)+\Delta I_3(0)\Delta I_2(t)\rangle\;, \tag{4.5}$$

with $\Delta I(t)=I(t)-\langle I(t)\rangle$. From Ref. 2, when $\mu_{23}<\mu_{12}$ and at zero temperature, one obtains:

$$\begin{aligned} S_{23}^{S}(\omega) \;=\; & -\frac{e^2}{2\pi}|\omega|(T_{21}T_{13}-(2-R_2-R_3)T_{23}) \\ & -\frac{e^2}{2\pi\hbar}\begin{cases} +T_{23}R_2\mu_{23}+T_{13}R_3\mu_{13}+T_{12}R_2\mu_{12} & \text{if } |\hbar\omega|<\mu_{23} \\ \hbar|\omega|(T_{23}R_2)+T_{13}R_3\mu_{13}+T_{12}R_2\mu_{12} & \text{if } \mu_{23}<|\hbar\omega|<\mu_{12} \\ \hbar|\omega|(T_{12}R_2+T_{23}R_2)+T_{13}R_3\mu_{13} & \text{if } \mu_{12}<|\hbar\omega|<\mu_{13} \\ \hbar|\omega|(T_{13}R_3+T_{12}R_2+T_{23}R_2) & \text{if } \mu_{13}<|\hbar\omega| \end{cases} \end{aligned} \tag{4.6}$$

The frequency dependence of $S_{23}^{S}(\omega)$ is symmetric in ω. The non-symmetrized cross-correlations, given by Eqs. (4.2) and (4.3), coincides with the symmetrized cross-correlations at $\omega=0$, as illustrated in Fig. 3. The non-symmetrized cross-correlations behavior is quite different from the symmetrized cross-correlations, although the locations of their singularities are the same. The symmetrized and non-symmetrized cross-correlations are both negative. The non-symmetrized cross-correlations are monotonously increasing and equal to zero for $\hbar\omega>\mu_{13}$.

We now consider the measured cross-correlations, given by Eq. (3.9), as a function of temperature of the measurement circuit. Because of the symmetry of the transmission probabilities, we have $S_{23}^{\pm}(\omega)=S_{32}^{\pm}(\omega)$. Note that positive frequencies correspond to an emission rate from the mesoscopic device in $S_{23}^{+}(\omega)$, while they correspond to an absorption rate in $S_{23}^{-}(\omega)$ [6, 12]. With the above symmetry consideration, the charge fluctuations resemble the formula for auto-correlation noise:

$$\langle x^2(0)\rangle=\frac{\alpha_1\alpha_2\pi}{(\Omega M)^2}[S_{23}^{+}(\omega)+\Delta S_{23}(\omega)N(\omega)]\;. \tag{4.7}$$

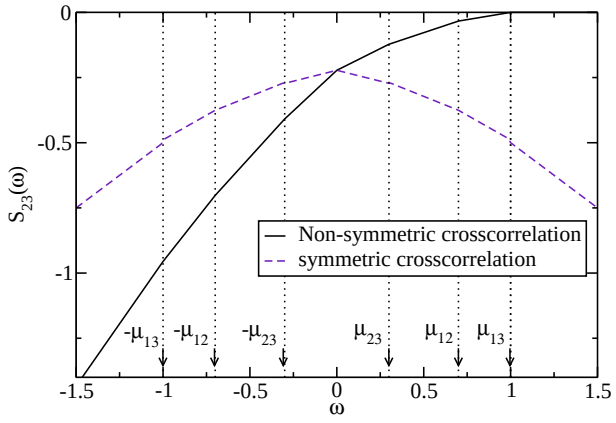

FIG. 3: Comparison between non-symmetrized and symmetrized cross-correlations as a function of frequency for $\mu_{12} > \mu_{23}$, in units of $e^2\mu_{13}/2\pi\hbar$. Singularities occur at $\hbar\omega = 0$, $\pm\mu_{23}$, $\pm\mu_{12}$, $\pm\mu_{13}$. The curves are plotted for $\mu_{12} = 0.7\mu_{13}$ and $\mu_{23} = 0.3\mu_{13}$.

Note that it is the difference of the two non–symmetrized correlators $\Delta S_{23}(\omega) = S^+_{23}(\omega) - S^+_{23}(-\omega)$ which is multiplied by the Bose distribution $N(\omega)$:

$$\Delta S_{23}(\omega) \;=\; -\frac{e^2}{2\pi}\omega\Big(T_{21}T_{13} - (2 - R_2 - R_3)T_{23} \\ -2T_{13}R_3 - 2T_{12}R_2 - 2T_{23}R_2\Big)\;, \tag{4.8}$$

i.e., it is linear with frequency with a positive slope, and does not have any singularities.

Taking $\mu_2 = \mu_3$ for simplicity, the measured cross-correlations are plotted in Fig. 4.

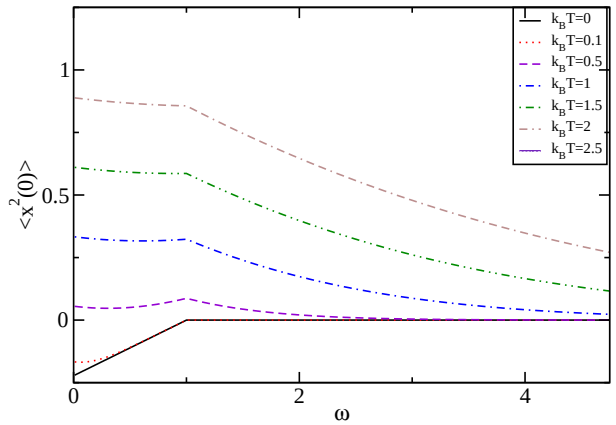

FIG. 4: Measured charge fluctuations as a function of frequency for different temperatures k_BT, measured in units of μ_{13}. The frequency and the biases are in units of μ_{13}.

For temperatures such that $k_BT \gg \nu_{\dots}$ the Bose distribution is large, $N(\omega) \sim k_BT/\hbar\omega \gg$

1. $\Delta S_{23}(\omega)N(\omega)$ is thus larger than $|S_{23}^{+}(\omega)|$. The effect of the increasing temperature is to change the sign of the charge fluctuations which become positive. This may seem change given the fact that one is computing the fluctuations of charge at the plates of a capacitor: recall that our measurement implicitly assumes two experiments with different wiring, whose results are subtracted one from another. The main message of Fig. 4 is that the sign of the measured correlation can be misleading if the temperature of the measuring device is too large: one can observe positive cross-correlations in a normal fermionic fork although this is a system where anti-bunching is expected. For $\omega \geq \mu_{13}$, the measured noise equals $\Delta S_{23}(\omega)N(\omega)$, while for $\omega < \mu_{13}$, $S_{23}^{+}(\omega)$ lowers $\Delta S_{23}(\omega)N(\omega)$. At all temperatures, the measured charge fluctuations have a clear singularity at $\hbar\omega = \mu_{13}$: we are not taking into account the thermal effects in the mesoscopic circuit itself.

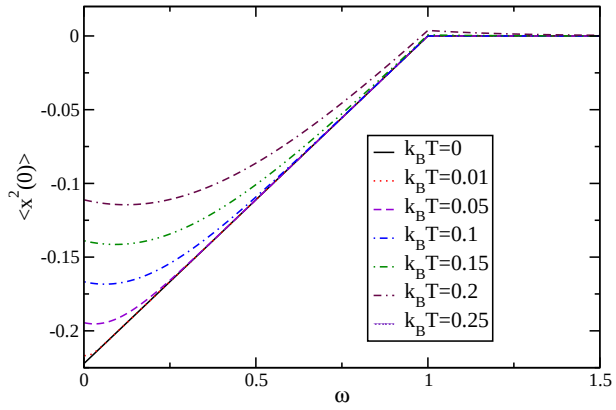

FIG. 5: Same as Fig. 4, for a smaller frequency range and at lower temperatures (in units of μ_{13}).

At low temperature, $k_B T \ll \mu_{13}$, and low frequency, $\omega \ll \mu_{13}$, $\Delta S_{23}(\omega)N(\omega)$ is smaller than $|S_{23}^{+}(\omega)|$ and the measured signal remains negative (see Fig. 5). When the temperature goes to zero, the measured charge fluctuations equal $S_{23}^{+}(\omega)$.

For completeness, the case where the voltage biases satisfy $\mu_{13} > \mu_{12} > \mu_{23} > 0$ is discussed. The fact that terminals 2 and 3 have different chemical potential will lower the contribution of $S_{23}^{+}(\omega)$ to $\Delta S_{23}(\omega)N(\omega)$, and increase the amplitude of charge fluctuations. At low temperature, the charge fluctuations stay negatives and singularities are present at frequencies equal to μ_{23}, μ_{12}, μ_{13}. When the temperature becomes larger than the bias voltages, the charge fluctuations become positive. However, when the temperature goes to zero, the charge fluctuation become equal to $S_{23}^{+}(\omega)$. When the difference between the chemical

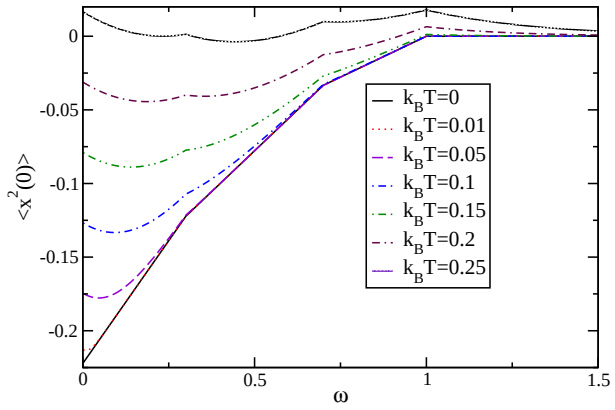

FIG. 6: Same as Fig. 4, for a smaller frequency range, and at lower temperatures. $\mu_{12} = 0.7\mu_{13}$, $\mu_{23} = 0.3\mu_{13}$ have been chosen.

temperature the amplitude is bigger regardless of the effect of $S^{+}_{23}(\omega)$ is less important for large temperatures.

V. WHEN ARE FINITE FREQUENCY NOISE CROSS-CORRELATIONS USEFUL ?

When probing quantum non-locality with a source of electrons (for instance a S–wave superconductor or any other source of electrons) with the help of Bell inequalities[17], one is confronted with the fact that particle number correlators must be converted into noise correlators. The particle number operator reads:

$$N_\alpha(\tau) = \int_0^\tau I_\alpha(t')dt' = \langle N_\alpha(\tau)\rangle + \delta N_\alpha(\tau) \ , \tag{5.1}$$

where $I_\alpha(t)$ is the current operator in lead α. The irreducible particle number correlator is expressed in terms of the finite frequency shot noise power:

$$\langle \delta N_\alpha(\tau)\delta N_\beta(\tau)\rangle = (1/2\pi)\int_{-\infty}^{\infty} d\omega S_{\alpha,\beta}(\omega) 4\sin^2(\omega\tau/2)/\omega^2 \ . \tag{5.2}$$

It is therefore only in the limit of relatively "large" acquisition times that the Bell inequality can be cast in terms of zero frequency correlations only[17, 18], thus the need in general to measure in general finite frequency noise correlations. This is implicit in the work of Ref. 19, where entanglement occurs with a normal source of electrons, provided that short time dynamics can be analyzed. Ref. 17 missed this subtlety concerning normal electron

Another situation of interest for finite frequency noise cross-correlations deals with the detection of anomalous (non-integer charges) in carbon nanotube. A Hanbury–Brown and Twiss experiment has been proposed where an STM tip injects electron in the bulk of the nanotube and noise cross-correlations are measured at the extremities of the nanotube[11, 20]. In Ref. 20, the case of an infinite nanotube has been considered. Schottky-like relations for the zero-frequency Fourier transforms of the auto-correlation noise and the cross-correlations noise were derived within the Tomonaga-Luttinger model:

$$S_{auto}(\omega = 0) = \frac{1 + (K_{c+})^2}{2} e|\langle I(x)\rangle| \ , \tag{5.3}$$

$$S_{cross}(\omega = 0) = \frac{1 - (K_{c+})^2}{2} e|\langle I(x)\rangle| \ , \tag{5.4}$$

where $\langle I(x)\rangle$ is the charge current through the nanotube and K_{c+} is the Luttinger liquid interaction parameter. S_{auto} is the term of auto-correlations and S_{cross} is the cross-correlations term. However, in the presence of electrical contacts at the extremities of the nanotube, the zero-frequency Fourier transforms for noise and cross-correlations lose their K_{c+}-dependence: at order 2 in the perturbative expansion with the tunneling amplitude from the tip to the nanotube, they reduce to $S_{auto}(\omega = 0) = e|\langle I(x)\rangle|$ and $S_{cross}(\omega = 0) = 0$. It has been shown in Ref. [11], that one has to consider finite frequency Fourier transform in order to recovered non zero cross-correlations and coulomb interactions effects in such a system.

VI. CONCLUSION

In summary, we have shown that the noise cross-correlations of a mesoscopic circuit can be measured by coupling the latter to a resonant circuit composed of and a capacitor. Each inductance is attached to the arms where correlations are measured. As in Ref. [6], the diagnosis of the noise is made by measuring the charge fluctuations on the capacitor. Two distinct measurements, with different wiring of the circuit, are necessary to isolate the noise cross-correlations.

Note that the quality of the diagnosis of cross-correlations presented in this work depends to a large extent on how the mesoscopic circuit is perturbed when one switches from one wiring configuration to the other. Indeed, it is necessary to minimize the changes in configuration (the values of α_1 and α_2) of the circuit which occurs between the two measurements. Here one assumes that the inductances are built "on chip" with the mesoscopic circuit, or

with the wires connected to it, and that the wires of the measurement circuit have a low impedance compared to that of the mesoscopic sample: within these working conditions the change of wiring does not affect significantly the inductive couplings, and the measurement will be reliable.

As a first necessary application of this measurement scheme, we considered a three terminal normal metal conductor, which is known to exhibit negative noise correlations at zero frequency. The symmetrized noise differs strongly from the non-symmetrized noise and the measured noise. For a mesoscopic circuit at zero temperature, the non-symmetrized noise contains singularities at frequencies corresponding to the chemical potential differences. However, when considering the measured noise, care must be taken to work with a detector circuit whose temperature is below these relevant biases. In this case the singularities in the derivative can still be detected, and upon increasing slowly the temperature, the measured noise deviates from the non-symmetrized noise. This sets a working condition for the observation of negative noise correlations – electron anti-bunching – in such three terminal devices. Another point is that we have neglected any amplification stages around the mesoscopic device in the electronic circuit, which could further increase the amplitude of the detected signal. Because of the above mentioned temperature effects of the device, such amplifiers would need to be cooled down.

The present analysis can be extended to study the measured noise correlations in other mesoscopic devices, in particular three terminal structures where electrons are injected in one lead from a superconductor[21]. Finite frequency noise correlations in this case contain information of the time dynamics of the two electrons subject to crossed-Andreev transport.

VII. APPENDIX

We discuss the case where the resonant LC circuit has a finite line shape. For a distribution of oscillators, the charge operator now takes the form:

$$x(t) = \sum_{\omega} x_{\omega}(t) = \sum_{\omega} \sqrt{\hbar/2M\omega}(a_{\omega}e^{-i\omega t} + a_{\omega}^{\dagger}e^{i\omega t}) \ , \tag{7.1}$$

where the interaction coupling, $\alpha \dot{I} x$, becomes $\dot{I} \sum_{\omega} \alpha_{\omega} x_{\omega}$.

These expressions are substituted in the interlocked commutators Eq. (2.9), which now contains a sum over 4 frequencies ω_1, ω_2, ω_3 and ω_4. Because of time integrations, delta

functions appear and give equalities between the frequencies. We are left with two summations:

$$\begin{aligned}
&\left\langle \left[[x^2(0), x(t_1)\dot{I}_i(t_1)], x_(t_2)\dot{I}_j(t_2) \right] \right\rangle = \\
&\sum_{\omega_1,\omega_2} \frac{2\hbar^2}{(2M)^2\omega_1\omega_2}(e^{i\omega_1 t_1} - e^{-i\omega_1 t_1}) \\
&\times \Big[\langle \dot{I}_i(t_1)\dot{I}_j(t_2)\rangle (N_{\omega_2} e^{-i\omega_2 t_2} + (N_{\omega_2}+1)e^{i\omega_2 t_2}) \\
&- \langle \dot{I}_j(t_2)\dot{I}_i(t_1)\rangle ((N_{\omega_2}+1)e^{-i\omega_2 t_2} + N_{\omega_2} e^{i\omega_2 t_2}) \Big] \ . \qquad (7.2)
\end{aligned}$$

We substitute this expression in the charge fluctuations and proceed with the change of variable, make use of the time translational invariance: $t = t_1 - t_2$ and $T = t_1 + t_2$ and $\langle I_i(t) I_j(0)\rangle = \langle I_i(0) I_j(-t)\rangle$. Making use of the definitions of Eqs. (3.7) and (3.8), the integral over T leads to two contributions:

$$\begin{aligned}
K_1 &= \int_{-\infty}^{0} dT e^{i(\omega_1+\omega_2)t/2} e^{\eta T + i(\omega_1-\omega_2)sign(t)T/2} \ , \\
&= \frac{e^{i(\omega_1+\omega_2)t/2}}{\eta + i(\omega_1-\omega_2)sign(t)/2} \qquad (7.3) \\
K_2 &= -\int_{-\infty}^{0} dT e^{i(-\omega_1+\omega_2)t/2} e^{\eta T - i(\omega_1+\omega_2)sign(t)T/2} \\
&= -\frac{e^{i(-\omega_1+\omega_2)t/2}}{\eta - i(\omega_1+\omega_2)sign(t)/2} \ . \qquad (7.4)
\end{aligned}$$

The line shape $L(\omega - \Omega)$, which is sharply peak around the resonant circuit frequency Ω, is introduced when converting discreet sums over frequencies into integrals. The integral over t is performed subsequently.

The denominators of K_1 and K_2 yield a real part which are a principal part and a imaginary part which are a Dirac delta function. We obtain four contributions for the charge fluctuations:

$$\langle x^2(0)\rangle = A_1 + A_2 + A_3 + A_4 \ , \qquad (7.5)$$

where

$$
\begin{aligned}
A_1 &= 2\pi^2 \int d\omega L^2(\omega-\Omega)\frac{\alpha_1\alpha_2}{(2M)^2} \\
&\times \left[(N_\omega+1)(S_{12}^+(\omega)+S_{21}^+(\omega))\right. \\
&\left. -N_\omega(S_{12}^-(\omega)+S_{21}^-(\omega))\right] \ , \qquad (7.6) \\
A_2 &= -\int d\omega_1 d\omega_2 d\omega_3 L(\omega_1-\Omega)L(\omega_2-\Omega)\frac{\omega_3^2}{\omega_1\omega_2}\frac{\alpha_1\alpha_2}{(2m)^2} \\
&\times \mathcal{P}\Big(((\omega_1+\omega_2)/2-\omega_3)^{-1}\Big)\mathcal{P}\Big(2/(\omega_1-\omega_2)\Big) \\
&\times \left[(N_{\omega_2}+1)(S_{12}^+(\omega_3)+S_{21}^+(\omega_3))\right. \\
&\left. -N_{\omega_2}\Big(S_{12}^-(\omega_3)+S_{21}^-(\omega_3)\Big)\right] \ , \qquad (7.7) \\
A_3 &= 2\pi^2 \int d\omega L(\omega-\Omega)L(-\omega-\Omega)\frac{\alpha_1\alpha_2}{(2m)^2} \\
&\times \left[(N_\omega+1)(S_{12}^+(-\omega)+S_{21}^+(-\omega))\right. \\
&\left. -N_\omega(S_{12}^-(-\omega)+S_{21}^-(-\omega))\right] \ , \qquad (7.8) \\
A_4 &= -\int d\omega_1 d\omega_2 d\omega_3 L(\omega_1-\Omega)L(\omega_2-\Omega)\frac{\omega_3^2}{\omega_1\omega_2}\frac{\alpha_1\alpha_2}{(2m)^2} \\
&\times \mathcal{P}\Big(((\omega_1-\omega_2)/2-\omega_3)^{-1}\Big)\mathcal{P}\Big(2/(\omega_1+\omega_2)\Big) \\
&\times \left[(N_{\omega_2}+1)(S_{12}^+(\omega_3)+S_{21}^+(\omega_3))\right. \\
&\left. -N_{\omega_2}\Big(S_{12}^-(\omega_3)+S_{21}^-(\omega_3)\Big)\right] \ , \qquad (7.9)
\end{aligned}
$$

where the fonction $\mathcal{P}$ gives the principal part. The contribution which dominates is the contribution where the two line shape functions $L(\omega-\Omega)$ are peaked at the same frequency, i.e., Eq (7.6). The quantity η which appears in the single oscillator model thus corresponds physically to the width of the line shape, as expected.

---

[1] S.R. Eric Yang, Solid State Commun. **81**, 375 (1992).

[2] Y.M. Blanter and M. Büttiker, Phys. Rep. **336**, 1 (2000).

[3] J. Torrès, T. Martin, and G. Lesovik Phys. Rev. B **63**, 134517 (2001).

[4] C. Chamon, D. E. Freed, and X. G. Wen, Phys. Rev. B **53**, 4033 (1996).

[5] T. Martin and R. Landauer, Phys. Rev. B **45**, 1742 (1992); M. Büttiker, Phys. Rev. B **45**, 3807 (1992).

[6] G. B. Lesovik and R. Loosen, Pis'ma Zh. Éksp. Teor. Fiz. **65**, 280 (1997) [JETP Lett. **65**,

[7] R. Aguado and L. Kouwenhoven, Phys. Rev. Lett. **84**, 1986 (2000).

[8] R. Deblock, E. Onac, L. Gurevich, and L. P. Kouvenhoven, Science **301**, 203 (2003).

[9] G. B. Lesovik, T. Martin, and G. Blatter, Eur. Phys. J. B. **24**, 287 (2001).

[10] P. Recher, E.V. Sukhorukov, and D. Loss, Phys. Rev. B **63**, 165314 (2001).

[11] A. V. Lebedev, A. Crépieux, and T. Martin, Phys. Rev. B **71**, 075416 (2005).

[12] Y. Gavish, I. Imry, and Y. Levinson, Phys. Rev. B **62**, 10637 (2000).

[13] G. B. Lesovik, A. V. Lebedev, and G. Blatter, Phys. Rev. B **71**, 125313 (2005).

[14] R. Hanbury-Brown and R. Q. Twiss, Nature **177**, 27 (1956).

[15] M. Henny, S. Oberholzer, C. Strunk, T. Heinzel, K. Ensslin, M. Holland, and C. Schönenberger, Science **284**, 296 (1999); W. D. Oliver, J. Kim, R. C. Liu, and Y. Yamamoto, Science **284**, 299 (1999).

[16] T. Martin in Les Houches Summer School session LXXXI, edited by E. Akkermans, H. Bouchiat, S. Gueron, and G. Montambaux (Springer, 2005).

[17] N. Chtchelkatchev, G. Blatter, G. Lesovik, and T. Martin, Phys. Rev. B **66**, 161320 (2002).

[18] C. W. J. Beenakker, C. Emary, M. Kindermann, and J. L. van Velsen, Phys. Rev. Lett **91**, 147901 (2003); C. W. J. Beenakker and M. Kindermann, Phys. Rev. Lett **92**, 056801 (2004); P. Samuelsson, E. V. Sukhorukov, and M. Buttiker, Phys. Rev. Lett **91**, 157002 (2003); P. Samuelsson, E.V. Sukhorukov, and M. Büttiker Phys. Rev. Lett. **92**, 026805 (2004).

[19] A. V. Lebedev, G. B. Lesovik, and G. Blatter, Phys. Rev. B **71**, 045306 (2005).

[20] A. Crépieux, R. Guyon, P. Devillard, and T. Martin, Phys. Rev. B **67**, 205408 (2003).

[21] J. Torrès and T. Martin, European Phys. J. B **12**, 319 (1999).